Inorganic Chemistry

Article

pubs.acs.org/IC

Zinc(II) Interactions with Brain-Derived Neurotrophic Factor N-Terminal Peptide Fragments: Inorganic Features and Biological Perspectives

Alessio Travaglia,[†] Diego La Mendola,*[,‡] Antonio Magrì,[§] Adriana Pietropaolo,[∥] Vincenzo G. Nicoletti,[⊥] Giuseppe Grasso,[+] Gaetano Malgieri,[◊] Roberto Fattorusso,[◊] Carla Isernia,[◊] and Enrico Rizzarelli[+]

[†]Center for Neural Science, New York University, 4 Washington Place, New York, New York 10003, United States

[‡]Dipartimento di Farmacia, Università di Pisa, Via Bonanno Pisano 6, 56126 Pisa, Italy

[§]Istituto di Biostrutture e Bioimmagini, Consiglio Nazionale delle Ricerche (CNR) Catania, Viale A. Doria 6, 95125 Catania, Italy

[∥]Dipartimento di Scienze della Salute, Università di Catanzaro, Viale Europa, 88100 Catanzaro, Italy

[⊥]Dipartimento di Scienze Biomediche and [+]Dipartimento di Scienze Chimiche, Università degli Studi di Catania, Viale A. Doria 6, 95125 Catania, Italy

[◊]Dipartimento di Scienze e Tecnologie Ambientali, Biologiche e Farmaceutiche, Seconda Università di Napoli, Via A. Vivaldi 43, 81100 Caserta, Italy

Supporting Information

ABSTRACT: Brain-derived neurotrophic factor (BDNF) is a neurotrophin essential for neuronal differentiation, growth, and survival; it is involved in memory formation and higher cognitive functions. The N-terminal domain of BDNF is crucial for the binding selectivity and activation of its specific TrkB receptor. Zn^{2+} ion binding may influence BDNF activity. Zn^{2+} complexes with the peptide fragment BDNF(1−12) encompassing the sequence 1−12 of the N-terminal domain of BDNF were studied by means of potentiometry, electrospray mass spectrometry, NMR, and density functional theory (DFT) approaches. The predominant Zn^{2+} complex species, at physiological pH, is [ZnL] in which the metal ion is bound to an amino, an imidazole, and two water molecules (NH_2, N_{Im}, and $2O_{water}$) in a tetrahedral environment. DFT-based geometry optimization of the zinc coordination environment showed a hydrogen bond between the carboxylate and a water molecule bound to zinc in [ZnL]. The coordination features of the acetylated form [AcBDNF(1−12)] and of a single mutated peptide [BDNF(1−12)D3N] were also characterized, highlighting the role of the imidazole side chain as the first anchoring site and ruling out the direct involvement of the aspartate residue in the metal binding. Zn^{2+} addition to the cell culture medium induces an increase in the proliferative activity of the BDNF(1−12) peptide and of the whole protein on the SHSY5Y neuroblastoma cell line. The effect of Zn^{2+} is opposite to that previously observed for Cu^{2+} addition, which determines a decrease in the proliferative activity for both peptide and protein, suggesting that these metals might discriminate and modulate differently the activity of BDNF.

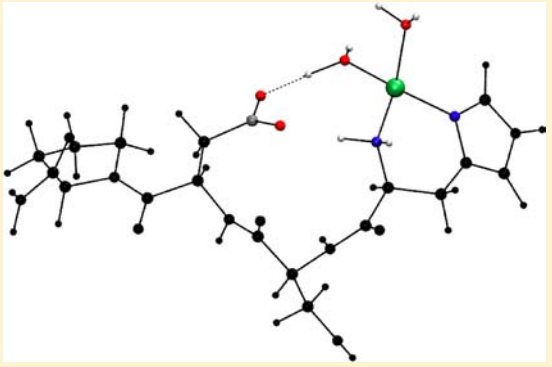

INTRODUCTION

Brain-derived neurotrophic factor (BDNF) is a member of the neurotrophin family, secreted proteins essential for survival and wiring regulation of the central and peripheral nervous system.[1,2] Like other neurotrophins, BDNF is synthesized as a precursor (pro-BDNF) and cleaved by proteases to produce the C-terminal mature and active form, which exerts its biological action as a noncovalent homodimer.[3,4] BDNF exerts its activity through interaction with two distinct classes of receptors: tropomyosin receptor kinase B (TrkB), responsible for prosurvival activity, and the p75 receptor, which is involved in apoptotic pathways.[5]

The expression, secretion, and activity of BDNF are controlled by neural activity, and the BDNF/TrkB system has a key function in the central nervous system, displaying multiple roles in different brain regions.[6,7] BDNF is neuroprotective in the hippocampus, particularly against ischemic damage,[8] preventing peroxide accumulation and increasing antioxidant enzymes.[9] It mediates energy metabolism and feeding behavior.[10] BDNF has a predominant role in higher cognitive functions, regulating the neurogenesis in the dentate gyrus of the hippocampus and in the subventricolar zone.[11−13] It influences neuronal plasticity, essential in the development of long-term potentiation (LTP)[14,15] and also through cAMP response element-binding protein (CREB) activation.[16,17]

Received: May 26, 2013
Published: September 26, 2013

   dx.doi.org/10.1021/ic401318t | *Inorg. Chem.* 2013, 52, 11075−11083

Chart 1. Sequence of a BDNF(1−12) Peptide[a]

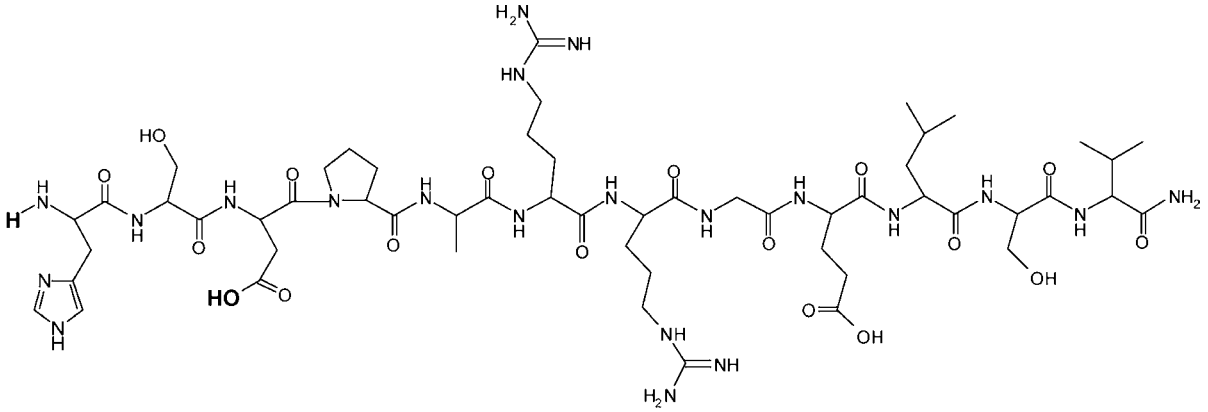

	$HSDPARRGELSV\text{-}NH_2$	BDNF(1-12)
H = Ac	$Ac\text{-}HSDPARRGELSV\text{-}NH_2$	Ac-BDNF(1-12)
OH = NH_2	$HSNPARRGELSV\text{-}NH_2$	BDNF(1-12)D3N

[a]In the acetylated pepide Ac-BDNF(1−12), the hydrogen (in bold) in the first residue is substituted by an acetyl group; in the mutated form BDNF(1−12)D3N, the hydroxyl group of the Asp 3 residue is substituted by NH_2.

Moreover, BDNF, through its receptor TrkB, influences the morphological development of neurons as well as their synaptic connectivity.[18]

A relevant number of neurodegenerative and neuropsychiatric disorders, characterized by abnormalities in synaptic plasticity, have been associated with deficits in BDNF functions.[19,20]

The reduced brain level of BDNF could contribute to the progressive atrophy and death of neuronal populations in the brains of patients affected by Alzheimer's diseases (AD).[21,22] Moreover, the reduction of both pro-BDNF and mature BDNF levels has been linked with loss of memory and learning capabilities.[23]

It is interesting to note that transition-metal ions are active in neuromodulation/neurotrasmission[24,25] and play an important role in the onset and progression of AD.[26−30] This is particularly relevant for glutamatergic synapses in the hippocampus, a region involved in learning and memory. More recently, metal ions have been suggested to be an essential component of memory formation together with neurons and the neural extracellular matrix.[31]

Zinc is abundant in the brain, and the majority is mostly tightly bound to proteins, such as metallothioneins and zinc-dependent transcription factors.[32] A fraction of zinc (∼10%) is free or loosely bound, and it is mainly localized in the presynaptic vesicles of zinc-containing neurons.[33] In response to neural activity, zinc stored in vesicles is released at the mossy fiber CA3 pyramidal synapses together with glutamate and may serve to modulate responses of *N*-methyl-D-aspartate (NMDA) receptors.[34,35] The hippocampus is one of the most zinc-enriched areas in the brain, and zinc release is essential for hippocampus-dependent learning, memory, and LTP.[36,37] In agreement with these findings, dietary zinc deficiency may induce learning and memory impairment.[38,39] Mice knockout of the specific zinc transporter ZnT3 showed a reduced activation of signaling pathways necessary for hippocampus-dependent memory.[40]

Interestingly, BDNF has been reported to increase the intracellular Zn^{2+} level in retinal pigment epithelium cells, modulating the expression of zinc transporters that increase metal-ion uptake.[41] Moreover, treatments with zinc(II) (or Zn^{2+}) ions induced the increase of BDNF expression in the cortex and hippocampus[42] and in mice models of AD disease,[43] strongly suggesting a reciprocal cross talk between metal-ion homeostasis and neurotrophin expression.

Metal ions can also modulate neurotrophin activities. Indeed, the BDNF treatment of cultured cortical neurons has been reported to affect TrkB phosphorylation in the presence of Zn^{2+} through the metal-induced extracellular activation of matrix metalloproteinase.[44,45] In addition, high concentrations of Zn^{2+} and Cu^{2+} have been reported to inhibit the effects of nerve growth factor (NGF) as well as BDNF, NT-3, and NT-4/5 in vitro.[46] These effects have been attributed to metal-induced conformational changes, which should alter the neurotrophin binding to a Trk receptor and the activation of its downstream pathways.[47]

Despite the fact that a large body of evidence suggests a cross-talk between BDNF and zinc, to the best of our knowledge, there is a lack of experimental data on the coordination features of BDNF-Zn complexes. Theoretical studies have proposed a model for neurotrophin/metal binding, suggesting that Zn^{2+} alters the conformation of NGF by forming a pentacoordinate complex. The same coordination environment has been proposed for BDNF-Zn.[48−50]

We had already ruled out that copper and zinc have the same coordination feature within the N-terminal domain of NGF.[51] More recently, we have experimentally characterized for the first time the coordination of Cu^{2+} and the BDNF N-terminal domain.[52]

The N-terminal residues of neurotrophins are crucial for the binding selectivity and activation of their respective Trk receptors.[46] For this reason, different peptide fragments have been synthesized in order to mimic whole neurotrophin activity.[51−55]

dx.doi.org/10.1021/ic401318t | *Inorg. Chem.* 2013, 52, 11075−11083

In the present paper, we report the characterization of Zn^{2+} complexes with the peptide fragment encompassing the N-terminal residues 1−12 of human BDNF [BDNF(1−12) = HSDPARRGELSV-NH_2, blocked at the C-terminus; Chart 1]. The Zn^{2+} complexes with BDNF(1−12) were studied by means of potentiometry, electrospray ionization spectrometry (ESI-MS), NMR, parallel tempering (PT) simulations, and density functional theory (DFT)-based geometry optimizations. The coordination features of the acetylated form [AcBDNF(1−12) = Ac-HSDPARRGELSV-NH_2], as well as of a single mutated peptide [BDNF(1−12)D3N = HSNPARRGELSV-NH_2], were also characterized to explore the involvement of specific donor groups.

Finally, the functional interactions of Zn^{2+} with BDNF peptides and with the whole protein were tested by measuring the effects on the proliferation rate of the SHSY5Y neuroblastoma cell line culture, and the obtained results were compared with those previously reported in the presence of Cu^{2+} ions.[52]

EXPERIMENTAL SECTION

Materials. NovaSyn-TGR resin, *N*-fluorenylmethoxycarbonyl (Fmoc)-protected amino acids, and 2-(1-*H*-benzotriazol-1-yl)-1,1,3,3-tetramethyluronium tetrafluoroborate (TBTU) were obtained from Novabiochem (Switzerland). *N*,*N*-Diisopropylethylamine (DIEA), *N*,*N*-dimethylformamide (peptide synthesis grade), piperidine, *N*-hydroxybenzotriazole (HOBT), triisopropylsilane, and trifluoroacetic acid (TFA) were purchased from Sigma-Aldrich. Deuterated D_2O (99.9% relative isotopic abundance) was purchased from Cambridge Isotope Laboratories. All the other chemicals were of the highest available grade and were used without further purification.

Peptide Synthesis and Purification. The peptides HSDPARRGELSV-NH_2 [BDNF(1−12)], Ac-HSDPARRGELSV-NH_2 [Ac-BDNF(1−12)], and HSNPARRGELSV-NH_2 [BDNF(1−12)D3N] were assembled using the solid-phase peptide synthesis strategy on a Pioneer peptide synthesizer as previously reported.[52] All amino acid residues were added according to the TBTU/HOBT/DIEA activation method for Fmoc chemistry. Other experimental details have already been reported.[52,56] The peptides were purified by means of preparative reversed-phase high-performance liquid chromatography (rp-HPLC) on a Varian PrepStar 200 model SD-1 chromatography system. Analytical rp-HPLC analysis was performed using an Agilent 1200 series instrument, using gradient elution with solvents A (0.1% TFA in water) and B (0.1% TFA in acetonitrile) on a Vydac C_{18} 250 × 4.6 mm (300 Å pore size, 5 μm particle size) column, at a flow rate of 1 mL/min. The peptides were eluted according to the following protocol: from 0 to 5 min, an isocratic gradient in 0% B, then a linear gradient from 0 to 15% B over 25 min, and finally an isocratic gradient in 15% B from 25 to 40 min. The peptides were characterized by means of ESI-MS.

HSDPARRGELSV-NH_2 [BDNF(1−12)]. R_t = 25.2 min. Calculated mass for $C_{54}H_{91}N_{21}O_{18}$ M = 1322.4. ESI-MS {obsd: m/z 1323.2 [$(M + H)^+$], 662.1 [$(M + 2H)^{2+}$]}.

Ac-HSDPARRGELSV-NH_2 [Ac-BDNF(1−12)]. R_t = 28.0 min. Calculated mass for $C_{56}H_{93}N_{21}O_{19}$ M = 1364.5. ESI-MS {obsd: m/z 1365.4 [$(M + H)^+$], 683.2 [$(M + 2H)^{2+}$]}.

HSNPARRGELSV-NH_2 [BDNF(1−12)D3N]. R_t = 34.2 min. Calculated mass for $C_{54}H_{92}N_{22}O_{17}$ M = 1321.5. ESI-MS {obsd: m/z 1322.4 [$(M + H)^+$], 661.7 [$(M + 2H)^{2+}$]}.

NMR Measurements. NMR sample solutions (2 mM) were prepared by dissolving the peptides in 90:10 (v/v) H_2O/D_2O. All the NMR spectra were recorded at 298 K using a Varian Unity 500 spectrometer, operating at 500 MHz. The proton chemical shifts were referenced to external tetramethylsilane (δ = 0 ppm). Bidimensional phase-sensitive TOCSY, NOESY, and ROESY[57] spectra were collected using the States and Haberkorn method; water suppression was achieved by the DPFGSE sequence.[58] A spectral width of 6000 Hz was used in both dimensions; typically, 4096 was the number of complex points collected in the ω_2 dimension and 512 in the ω_1 dimension; the data were zero-filled to 2 K in ω_1. Square-shifted sine-bell functions were applied in both dimensions *prior* to Fourier transformation and baseline correction. TOCSY, NOESY, and ROESY experiments were recorded with mixing times of 70, 300, and 180 ms, respectively. The data were processed and analyzed using the *VNMRJ* and *XEASY* software.[59] Zn^{2+} coordination was studied at a 1:1 peptide/Zn^{2+} molar ratio; the samples were prepared by adding a $ZnCl_2$/water solution (0.1 M) to the above-mentioned peptide solutions. Pulse-field-gradient (PFG) diffusion measurements with the pulse gradient-stimulated echo longitudinal encode−decode (PG-SLED) sequence[60] permitted to obtain D_{trans}, which is proportional to the decay rate of NMR signal attenuation as a function of the gradient strength. Each diffusion data set contained a series of 13 monodimensional ^1H NMR spectra with gradient strengths from 0.5 to 30 G/cm. For the obtainment of the translational diffusion coefficient D_{trans}, the DOSY package of the *VNMRJ* software was used.

Potentiometric Titrations. Potentiometric titrations were performed with two home-assembled fully automated apparatus sets (Metrohm E654 pH meter, combined with a micro-pH glass electrode, Orion 9103SC, and a Hamilton digital dispenser, model 665) controlled by the appropriate software setup in our laboratory. The titration cell (2.5 mL) was thermostated at 298.0 ± 0.2 K, and all solutions were kept under an atmosphere of argon, which was bubbled through a solution having the same ionic strength and temperature as the measuring cell. Potassium hydroxide (KOH) solutions (0.1 M) were added through a Hamilton buret equipped with 1 mL syringes.[61] The ionic strength of all solutions was adjusted to 0.10 M (KNO_3). To determine the stability constants, solutions of the ligands with Zn^{2+} were titrated by using 0.1 M KOH. The peptide concentration ranged from 1.0 to 3.0 × 10^{-3} M, and four independent experiments were run. The initial pH was always adjusted to 2.4, and titrations were performed in the pH range 2.5−7.0. A further increase of the pH value, at millimolar concentrations of peptide and metal ion, induces the formation of a precipitate due to hydrolytic species formation. Other details were as previously reported.[51] To obtain protonation and complexation constants, the potentiometric data were refined using the *HYPERQUAD* program,[62] which minimizes the error square sum of the measured electrode potentials through a nonlinear iterative refinement of the sum of the squared residuals, U, and also allows for the simultaneous refinement of data from different titrations:

$$U = \sum (E_{exp} - E_{calc})^2$$

E_{exp} and E_{calc} are the experimental and calculated electrode potentials, respectively. Errors in the stability constant values are reported as 3 times standard deviations. In data analysis, [ZnHL] complex species formation was also considered to refine the stability constant of main complex species.

The formation reaction equilibria of ligands with protons and Zn^{2+} ions are given in eq 1:

$$pZn + qH + rL = Zn_pH_qL_r \quad (1)$$

in which L are the peptides under study. The stability constant β_{pqr} is defined in eq 2:

$$\beta_{pqr} = [Zn_pH_qL_r]/[Zn]^p \cdot [H]^q \cdot [L]^r \quad (2)$$

The species distribution as a function of the pH was obtained by using the computer program *Hyss*.[63]

ESI-MS. ESI-MS measurements were carried out by using a Finnigan LCQ DECA XP PLUS ion-trap spectrometer operating in the positive-ion mode and equipped with an orthogonal ESI source (Thermo Electron Corp.). Water sample solutions were injected into the ion source at a flow rate of 5 μL/min, using nitrogen as the drying gas. The mass spectrometer operated with a capillary voltage of 46 V and a capillary temperature of 250 °C, while the spray voltage was 4.3 kV.

DFT Calculations. The starting coordinates of ^{1}HSDP^4, ^{1}Ac-HSDP^4, and ^{1}HSNP^4 domains were considered from the PT clusters

dx.doi.org/10.1021/ic401318t | *Inorg. Chem.* 2013, 52, 11075−11083

of BDNF(1−12), Ac-BDNF(1−12), and BDNF(1−12)D3N previously reported.[52] We selected the ^{1}HSDP^{4} section, adding a zinc ion. The N-terminal amine was acetylated for ^{1}Ac-HSDP^{4}, and the aspartate was mutated with asparagine for the ^{1}HSNP^{4} segment. All DFT calculations were performed using the *Gaussian 03* program[64] (revision D.02). The optimized geometries have been calculated using the B3LYP pseudopotential[65−68] and TZVP basis sets.[69,70] For all complexes, frequency calculations were performed to ensure that the geometries are local energy minima.

RESULTS AND DISCUSSION

BDNF(1−12), BDNF(1−12)D3N, and Ac-BDNF(1−12) Conformations. NMR measurements were carried out in water at pH 5.8. The narrow range of the HN resonance dispersion and the absence of secondary structure diagnostic NOEs[70] clearly confirm that the three peptides do not assume a definite conformation in these conditions (chemical shifts are reported in Table 1S in the Supporting Information), in agreement with the far-UV circular dichroism results previously reported.[52] Nevertheless, some differences among the three peptides' behavior emerge in a comparison of their chemical shifts. In fact, when the BDNF(1−12) peptide is acetylated, the backbone H_N chemical shifts of Asp3, Arg6, and Arg7 as well as the H_ε chemical shift of His1 appear slightly perturbed. This indicates that acetyl induces a local conformational backbone rearrangement involving these amino acids. In the case of BDNF(1−12)D3N, the chemical shift perturbations involve again the H_ε of His1 and the backbone H_N chemical shifts of Arg6 and Arg7, which, in turn, are also different compared to the chemical shifts of Ac-BDNF(1−12). These results are in agreement with the reported models of Travaglia et al.,[52] confirming the connection between His1, Asp3, Arg6, and Arg7 in the BDNF(1−12) peptide.

Speciation, Stability Constants, and Coordination Modes of Zn^{2+} Complexes with BDNF(1−12), BDNF(1−12)D3N, and Ac-BDNF(1−12). The stability constant values of the complexes of Zn^{2+} with BDNF(1−12), Ac-BDNF(1−12), and BDNF(1−12)D3N are listed in Table 1.

Table 1. Protonation and Stability Constants (log β_{pqr}) of Zn^{2+} Complexes for BDNF(1−12), BDNF(1−12)D3N, and Ac-BDNF(1−12) (T = 298 K, I = 0.10 M KNO_3)[a,b]

species (ZnHL)	BDNF(1−12)	Ac-BDNF(1−12)	BDNF(1−12)D3N
041	20.39(1)		
031	17.19(1)	14.07(1)	17.02(2)
021	12.97(1)	10.75(1)	12.99(2)
011	7.44(1)	6.44(1)	7.50(1)
111	9.49(6)		9.99(8)
101	5.18(1)	2.5(1)	5.36(1)

[a]Standard deviations (3σ values) are given in parentheses. [b]For protonation constants, see ref 52.

Acetylation of the terminal amino group simplifies the species distribution. In fact, Zn^{2+} does not form any complex with AcBDNF(1−12) up to pH 5, and above this pH only the $[ZnL]^{+}$ species forms (Figure 1).

The first species formed by BDNF(1−12) with the metal ion is $[ZnHL]^{2+}$, and its percentage of formation is very low, so it was not possible to characterize it by means of NMR measurements. However, the calculated stability constant value ($\log K_{(111)} = \log \beta_{(111)} - \log K_{(011)} = 2.05$) is very similar to that reported for the acetylhistidine amide ($\log \beta = 2.15$), a monodentate ligand having imidazole as its donor atom,[71]

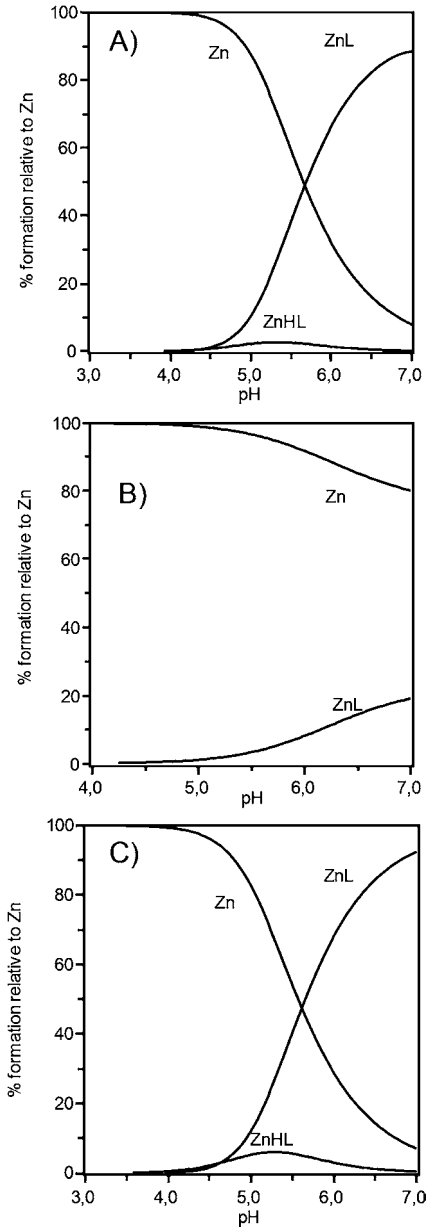

Figure 1. Species distribution diagram for Zn^{2+} complexes with (A) BDNF(1−12), (B) Ac-BDNF(1−12), and (C) BDNF(1−12)D3N. Charges are omitted for clarity. [L] = 1 × 10^{-3} mol dm^{-3}; M/L molar ratio of 1:1.

suggesting a similar $N_{Im}3O_{water}$ coordination mode. The stability constant value of BDNF(1−12)D3N is comparable to that reported for the analogous complex species [ZnHL] formed by histamine in which the imidazole nitrogen atom is bound to the metal-ion site and the amino group is still protonated.[72] The first complex species formed by Zn^{2+} with Ac-BDNF(1−12) is [ZnL]; its stability constant ($\log \beta = 2.5$) is equal to that found for the protonated species of Zn^{2+} with BDNF(1−12)D3N. Again, the stability constant is indicative of the involvement of the imidazole nitrogen atom, as found for complex species formed with analogous peptides.[71,73,74]

[ZnL] is the prevailing complex species for both BDNF(1−12) and BDNF(1−12)D3N at all pH ranges investigated (Figure 1). The stability constant values are higher than those of the related protonated species because of involvement of the amino group, which substitutes a water molecule in the Zn^{2+}

dx.doi.org/10.1021/ic401318t | Inorg. Chem. 2013, 52, 11075−11083

coordination sphere to form a six-membered chelate ring with involvement of the amino group and imidazole nitrogen atom (Figure 2).

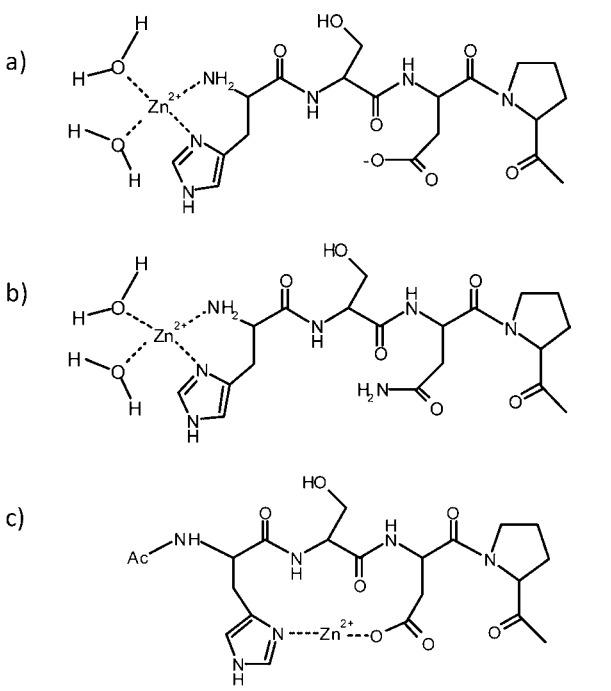

Figure 2. Schematic view of the [ZnL] complex species: (a) L = BDNF(1−12); (b) L = BDNF(1−12)D3N; (c) L = Ac-BDNF(1−12). In part c, metal-ion coordination environment is completed by water molecules (not shown).

This histamine-like coordination mode is indicative of the absence of a carboxylic group in metal binding.[75,76] A further evidence of this coordination mode results by the absence of analogous complex species in the acetylated peptide, in which the amino group is blocked (Figure 2). A further increase of the pH value induces precipitation due to hydrolytic species formation.[77]

The stoichiometry of zinc binding with the peptides was also investigated by ESI-MS.[78] The mass spectra obtained from an equimolar peptide and Zn^{2+} aqueous solution at pH 5.6 show that the percentages of the metal−peptide complexes relative to the free peptides are higher for BDNF(1−12) and BDNF(1−12)D3N (data not shown), while in the case of Ac-BDNF(1−12), the amount of metal complex is significantly lower, in agreement with the potentiometric data. The mass spectra carried out using 2 equiv of metal do not show the presence of bis-complex species.

NMR measurements were also carried out at pH 5.8, where the translational diffusion coefficients for BDNF(1−12), BDNF(1−12)D3N, and Ac-BDNF(1−12) remain unchanged upon Zn^{2+} addition (D_{trans}= 2.1 × 10^{-10} m^2 s^{-1}), ruling out metal-ion-mediated peptide−peptide aggregation phenomena within the NMR concentration range investigated. ^{1}H chemical shifts at a 1:1 peptide/Zn^{2+} molar ratio for BDNF(1−12), BDNF(1−12)D3N, and Ac-BDNF(1−12) are reported in Table 1S in the Supporting Information. The addition of Zn^{2+} to Ac-BDNF(1−12) did not result in significant chemical shift perturbations or signal broadening because of the very low metal complex formation percentage at this pH value, while the BDNF(1−12) and BDNF(1−12)D3N N-terminal residue resonances for His1 and (Asp/Asn)3 were either shifted and/or broadened upon Zn^{2+} addition.

The resonances assigned to H_ε and H_δ histidine imidazole rings shift upfield and broaden, with the H_ε signals experimenting the larger shift, while H_N and H_α of the residue in position 3 (Asp/Asn) disappear and its H_β chemical shifts show small but significant changes. These data clearly indicate that the His side chain is directly involved in the metal coordination in both peptides, while the substitution of Asp with the Asn residue does not induce relevant differences in the peptide coordination behavior. Comparable changes in the side-chain proton resonances of both peptides rule out the direct involvement of the aspartate residue in metal binding. However, a significant influence on the peptide conformations balance is evidenced by the highlighted modification of the backbone signals. The effect is particularly evident in the BDNF(1−12) peptide, where Arg6 and Arg7 backbone H_N resonances experience a downfield shift, thus reinforcing the hypothesis of a local conformation population rearrangement with respect to the free ligand.

Species distribution diagrams (Figure 1) show that the predominant complex species at pH 5.8 is the same as that found at pH 7. However, NMR measurements were also carried out at pH 7.0 as free ligands and in the presence of a 1:1 Zn^{2+}/peptide molar ratio (Table 3S in the Supporting Information). As expected, such a pH, because of the unfolded nature and exchange rates of the peptides, negatively influenced the quality of the NMR spectra (the signals sensitively broaden), so that they allowed only an incomplete assignment. The obtained data permitted anyhow to draw general and qualitative conclusions: the observed behavior of the two peptides is consistent with the behavior observed at pH 5.6, where the quality of the spectra is definitely more suitable for a complete NMR characterization.

DFT Coordination Polyhedra of a Zinc Ion Bound to ^{1}HSDP^4, ^{1}Ac-HSDP^4, and ^{1}HSNP^4 BDNF Fragments. DFT-based geometry optimizations were carried out on the main clusters of BDNF(1−12), Ac-BDNF(1−12), and BDNF(1−12)D3N obtained from the PT simulations reported in ref 52. From those, we selected the ^{1}HSDP^4, ^{1}Ac-HSDP^4, and ^{1}HSNP^4 domains in order to disclose the coordination geometries in [ZnL] species formed by the three peptides and how Zn^{2+} may induce different local conformations. The coordination polyhedron parameters of a zinc ion encompassing the N-terminal domain of BDNF are reported in Table 2S in the Supporting Information. Acetylation of the N-terminal amine, as well as the D3N mutation, was considered in order to validate the structural differences by replacing one N-terminal amine and one carboxylate. The minimum-energy structures of the former complexes predicted through DFT are reported in Figures 3−5.

All of the complexes adopt a distorted tetrahedral arrangement with marked differences among the three complexes. The coordination of the zinc ion in the ^{1}HSDP^4 sequence of a wild-type BDNF domain involves the N-terminal amine, the N_δ nitrogen of histidine, and two water molecules. A hydrogen bond connects one of the two water molecules with the aspartate (Figure 3), with a "stiffening effect" that can negatively influence metal complex formation because of the unfavorable entropy contribution.

Coordination of a zinc ion in the ^{1}Ac-HSDP^4 sequence of an acetylated BDNF domain involves one oxygen from aspartate, one oxygen from the histidine carbonyl, the N_δ nitrogen atom of histidine, and one water molecule (Figure 4).

dx.doi.org/10.1021/ic401318t | Inorg. Chem. 2013, 52, 11075−11083

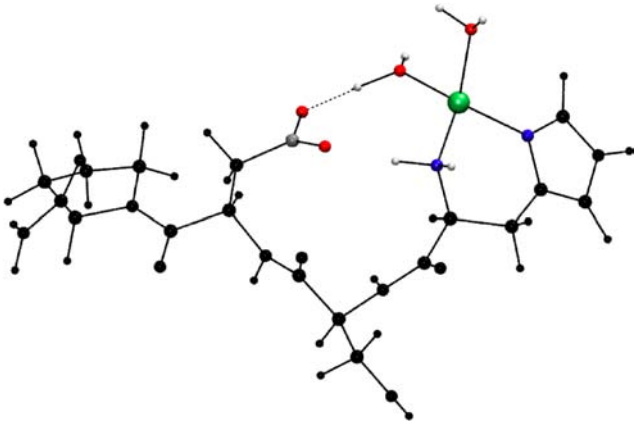

Figure 3. Coordination polyhedron of a zinc ion in the ^{1}HSDP^{4} domain of BDNF. The zinc ion is shown in green, nitrogens are in blue, oxygens are in red, and the BDNF backbone is shown as black spheres.

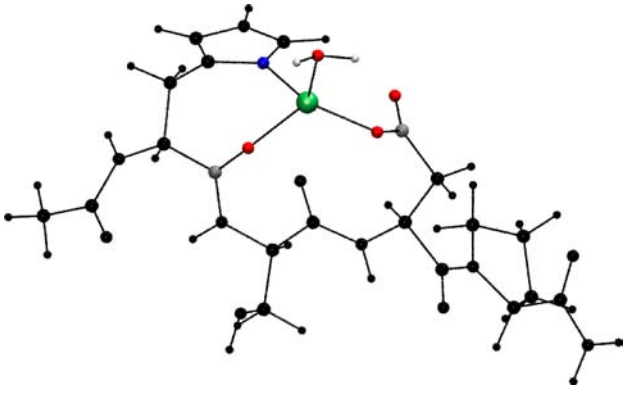

Figure 4. Coordination polyhedron of a zinc ion in the Ac-^{1}HSDP^{4} domain of Ac-BDNF(1−12). The zinc ion is shown in green, nitrogens are in blue, oxygens are in red, and the BDNF backbone is shown as black spheres.

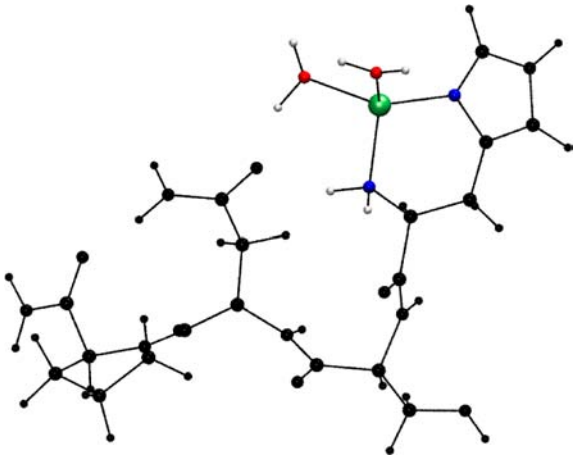

Figure 5. Coordination polyhedron of a zinc ion in ^{1}HSNP^{4} of BDNF(1−12)D3N. The zinc ion is shown in green, nitrogens are in blue, oxygens are in red, and the BDNF backbone is shown as black spheres.

Coordination of a zinc ion in the ^{1}HSNP^{4} sequence of the D3N-mutated BDNF involves, as the wild-type polyhedron, the N-terminal amine, the N_{δ} nitrogen of histidine, and two water molecules (Figure 5).

A comparison between the results pertinent to the ^{1}HSDP^{4} and ^{1}HSNP^{4} fragments allows to single out that the simultaneous coordination of the N-terminal amine and the N_{δ} nitrogen of histidine hampers access of the aspartate in the zinc coordination site (Figures 3 and 4), resulting in the absence of the aspartate residue inside the coordination shell, in agreement with potentiometric and NMR results. However, the aspartate group still interacts with the coordination site through hydrogen bonding with the first-shell water (Figure 3). Such an interaction is evident from the closer Zn−O_{w1} distance of the BDNF wild-type than that found in the BDNF-D3N mutant (Table 2S in the Supporting Information). Intriguingly, when the aspartate is mutated in asparagine, the $CONH_2$ group turns out backward in the coordination site (Figure 5). The side-chain carbonyl group of N3 is hydrogen-bonded to coordination water with a distance of 1.58 Å, while the amide group of N3 is hydrogen-bonded to the carbonyl of P4 with a distance of 1.78 Å. As found for the wild-type BDNF, also these hydrogen bonds stiffen the carbonyl of asparagine. The former carbonyl is oriented in the same manner as that found in the aspartate analogue. However, the presence of two hydrogen bonds in the asparagine side chain, one of the two involving the carbonyl of proline outside the coordination shell, can explain the slight increase of the [ZnL] stability constant formed with BDNF(1−12)D3N in comparison to that of BDNF(1−12) peptide.

Proliferative Effects of Zinc Complexes with BDNF Protein and Its N-Terminus Peptide Fragments on SHSY5Y Cells. The effect of Zn^{2+} ions on the proliferative effect of BDNF(1−12), BDNF(1−12)D3N, and Ac-BDNF(1−12) peptides was tested on neuronal undifferentiated cell cultures (neuroblastoma SHSY5Y) at less than 60% confluence and compared to that obtained with the whole protein BDNF. We have previously reported an increase of the cell number following treatment with both BDNF protein and BDNF peptides.[52] We have already shown a different activity between BDNF(1−12) and its acetylated and mutated analogues, which has been rationalized in terms of specific intermolecular interaction with the TrkB receptor.

Zinc is an essential cofactor for cell proliferation, differentiation, and apoptosis through different pathways in different tissues and cell types.[79,80] For example, a decrease in the Zn^{2+} availability inhibits IMR-32 neuroblastoma cell proliferation.[81] In agreement with these findings, we found that Zn^{2+} displays a proliferative effect on neuroblastoma SHSY5Y cells.

The Zn^{2+} addition turned out to increase the proliferative effect due to BDNF(1−12) as well as that of the whole BDNF protein (Figure 6). A slight increase is observed also for the mutated peptide BDNF(1−12)D3N, while a decrease in the proliferative activity is found for the acetylated form.

ESI-MS measurements were also carried out to confirm the stoichiometry of Zn^{2+} complex species in the experimental conditions used in the biological assay (pH 7.4; 10^{-5} M analytical concentration of the ligand and metal) to overcome potentiometric measurement limits.[82] As a matter of fact, these last measurements were carried out at millimolar concentration, and the pH range investigated is limited because of hydrolytic species formation, in particular for the acetylated peptide AcBDNF(1−12), which has a lower stability constant in comparison with the other two peptides. The mass spectra obtained from aqueous solutions equimolar in peptide and zinc at pH 7.4 show that the percentages of the metal−peptide complex relative to the free peptides are 65%, 60%, and 35% for

dx.doi.org/10.1021/ic401318t | Inorg. Chem. 2013, 52, 11075−11083

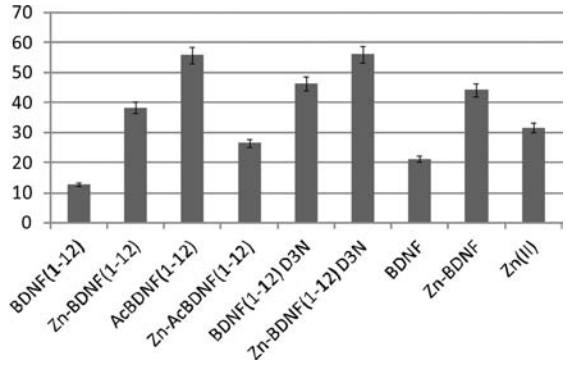

Figure 6. Proliferative effect, at 48 h, of BDNF(1−12) (10 μM) and the whole BDNF protein (10 nM) on neuroblastoma SHSY5Y cells in the absence and presence of Zn^{2+} ions (10 μM). The data are normalized with respect to control samples set to zero. One-way analysis of variance (ANOVA; P 0.05) was performed using the data from three to five independent experiments and a minimum of eight parallel runs for each experiment.

BDNF(1−12), BDNF(1−12)D3N, and AcBDNF(1−12), respectively. We can speculate that the similar effect on proliferation assay obtained by Zn^{2+} complexes with BDNF(1−12) and BDNF(1−12)D3N can be related to their similar metal coordination environments, whereas the analogous complex species formed by the acetylated form, having a different binding mode, display different activities, decreasing cell proliferation.

Conclusions. The role of BDNF, as well as of other neurotrophins, is essential in neuronal differentiation, growth, and survival. More recently, BDNF has been shown to be the neurotrophin most involved in the synaptic plasticity, memory formation, and higher cognitive functions. The release of zinc from synaptic vesicles is another essential factor for hippocampus-dependent learning and memory, although the mechanism through which the metal ion performs such activity remains incompletely understood. It is known that zinc can affect BDNF expression and/or activity, and this may represent a possible pathway to influence memory formation. Interestingly, zinc dyshomeostasis and the decrease of the BDNF levels are reported in AD patients that show a deficit in learning and memory as early symptoms.[21,22]

It has been reported that zinc and copper ions can affect the NGF activity through their binding to its N-terminal domain, which encompasses the residues involved in interaction with its specific Trk receptor, suggesting that a similar effect could be observed for other neurotrophins.[48−50]

Therefore, the direct Zn^{2+} binding to the N-terminal domain of BDNF protein may alter interaction with the TrkB receptor. Here, we report the characterization of Zn^{2+} complexes with the peptide fragment encompassing the N-terminal sequence 1−12 of BDNF by means of potentiometry, ESI-MS, NMR, and DFT geometry optimization.

We demonstrate that the predominant Zn^{2+} complex species, at physiological pH, is $[ZnL]^{2+}$, in which the metal ion is bound to one amino, one imidazole, and two water molecules (NH_2, N_{Im}, and $2O_{water}$) in a tetrahedral environment. A comparison with the analogous complex species formed by the acetylated peptide Ac-BDNF(1−12) and the single-point-mutated BDNF(1−12)D3N, in which the aspartate has been substituted by an asparagine residue, was helpful to clarify the essential role of the imidazole side chain as the first anchoring site of the metal and to rule out the direct involvement of the aspartate residue in metal binding.

DFT-based geometry optimizations of the zinc coordination environment highlight different hydrogen bonds in the [ZnL] species formed with BDNF(1−12) and BDNF(1−12)D3N, justifying the NMR behavior of backbone residues Asp/Asn in position 3. In particular, the hydrogen bond between the carboxylate and a water molecule bound to zinc in the Zn-BDNF(1−12) system and the hydrogen bond of the asparagine side chain with the contiguous proline carbonyl in the Zn-BDNF(1−12)D3N system furnishes evidence of the higher stability constant for the zinc complexes formed with single-point-mutated peptides.

The Zn^{2+} addition induces an increase in the proliferative activity of the BDNF(1−12) peptide at millimolar concentration and of the whole protein at nanomolar concentration. This indicates that the peptide fragment BDNF(1−12) is able to mimic the proliferative activity of the whole protein in the presence of metal ion. It is interesting to note that the effect of Zn^{2+} addition on the activity of BDNF(1−12) and the whole BDNF protein is opposite to that observed in the presence of Cu^{2+}, which causes a decrease in the proliferative activity for both peptide and protein.[52]

Interestingly, cell culture treatment with NGF in the presence of Cu^{2+} induced an increase and the Zn^{2+} addition caused a decrease in the proliferative activity.[51] The effect of metal ions is opposite to that observed for the BDNF protein.

Biological tests presented here indicate that copper and zinc, metals highly implicated in the biology and pathology of neurons, may discriminate and modulate differently the activity of the two most important neurotrophins, NGF and BDNF.

■ ASSOCIATED CONTENT

Supporting Information

^{1}H chemical shifts of BDNF(1−12), BDNF(1−12)D3N, and Ac-BDNF(1−12) as free ligands and in the presence of 1 equiv of Zn^{2+} (Table 1S; the data were collected in water at pH 5.8 and at 298 K), coordination parameters for Zn^{2+} polyhedra in ^{1}HSDP^4 [BDNF(1−12)], ^{1}Ac-HSDP^4 [AcBDNF(1−12)], and ^{1}HSNP^4 [BDNF(1−12)D3N] peptide fragments (Table 2S), ^{1}H chemical shifts of BDNF(1−12) and BDNF(1−12)D3N as free ligands and in the presence of 1 equiv of Zn^{2+} (Table 3S; the data were collected in water at pH 7.0 and at 298 K). This material is available free of charge via the Internet at http://pubs.acs.org.

■ AUTHOR INFORMATION

Corresponding Author

*E-mail: lamendola@farm.unipi.it. Tel.: +39(0)50 2219500. Fax: +39(0)50 2219605.

Notes

The authors declare no competing financial interest.

■ ACKNOWLEDGMENTS

MIUR (Rome) is gratefully acknowledged for partial support (PRIN 200993WWF9 to C.I. and PRIN 2010M2JARJ to D.L., R.F., and E.R.). Caspur Cluster is acknowledged for computational time provided under Project std12-149.

REFERENCES

(1) Leibrock, J.; Lottspeich, F.; Hohn, A.; Hofer, M.; Hengerer, B.; Masiakowski, P.; Thoenen, H.; Barde, Y. A. *Nature* **1989**, *341*, 149−152.
(2) Levi-Montalcini, R. *Science* **1987**, *237*, 1154−1162.
(3) Radziejewski, C.; Robinson, R. C.; Distefano, P. S.; Taylor, J. W. *Biochemistry* **1992**, *31*, 4431−4436.
(4) Pang, P. T.; Teng, H. K.; Zaitsev, E.; Woo, N. T.; Sakata, K.; Zhen, S.; Teng, K. K.; Yung, W.-H.; Hempstead, B. L.; Lu, B. *Science* **2004**, *306*, 487−491.
(5) Carter, B. D.; Kaltschmidt, C.; Kaltschmidt, B.; Offenhnauser, N.; Bohm-Matthaei, R.; Baeuerle, P. A.; Barde, Y. A. *Science* **1996**, *272*, 542−545.
(6) Park, H.; Poo, M. M. *Nat. Rev. Neurosci.* **2013**, *14*, 7−23.
(7) Chao, M. V. *Nat. Rev. Neurosci.* **2003**, *4*, 299−309.
(8) Larsson, E.; Nanobashvili, A.; Kokaia, Z.; Lindvall, O. *J. Cereb. Blood Flow Metab.* **1999**, *19*, 1220−1228.
(9) Mattson, M. P.; Lovell, M. A.; Furukawa, K.; Markesbery, W. R. *J. Neurochem.* **1995**, *65*, 1740−1751.
(10) Noble, E. E.; Billington, C. J.; Kotz, C. M.; Wang, C. *Am. J. Physiol.: Regul., Integr. Comp. Physiol.* **2011**, *300*, R1053−R1069.
(11) Benralss, A.; Chmielnicki, E.; Lerner, K.; Roh, D.; Goldman, S. A. *J. Neurosci.* **2001**, *21*, 6718−6731.
(12) Sairanen, M.; Lucas, G.; Ernfors, P.; Castren, M.; Castren, E. *J. Neurosci.* **2005**, *25*, 1089−1094.
(13) Bath, K. G.; Akins, M. R.; Lee, F. S. *Dev. Psychobiol.* **2012**, *54*, 578−589.
(14) Patterson, S. L.; Abel, T.; Deuel, T. A.; Martin, K. C.; Rose, J. C.; Kandel, E. R. *Neuron* **1996**, *16*, 1137−1145.
(15) Bekinschtein, P.; Cammarota, M.; Igaz, L. M.; Bevilaqua, L. R.; Izquierdo, I.; Medina, J. H. *Neuron* **2007**, *53*, 261−277.
(16) Chen, D. Y.; Bambah-Mukku, D.; Pollonini, G.; Alberini, C. M. *Nat. Neurosci.* **2012**, *15*, 1707−1714.
(17) Luine, V.; Frankfurt, M. *Neuroscience* **2013**, *239*, 34−45.
(18) Huang, E. J.; Reichardt, L. F. *Annu. Rev. Neurosci.* **2001**, *24*, 677−736.
(19) Arancio, O.; Chao, M. V. *Curr. Opin. Neurobiol.* **2007**, *17*, 325−330.
(20) Mattson, M. P. *Ann. N.Y. Acad. Sci.* **2008**, *1144*, 97−112.
(21) Hock, C.; Heese, K.; Hulette, C.; Rosenberg, C.; Otten, U. *Arch. Neurol.* **2000**, *57*, 846−851.
(22) Zuccato, C.; Cattaneo, E. *Nat. Rev. Neurol.* **2009**, *5*, 311−322.
(23) Peng, S.; Wuu, J.; Mufson, E. J.; Fahnestock, M. *J. Neurochem.* **2005**, *93*, 1412−1421.
(24) Xie, X. M.; Smart, T. G. *Nature* **1991**, *349*, 521−524.
(25) Bozym, R. A.; Thompson, R. B.; Stoddard, A. K.; Fierke, C. A. *ACS Chem. Biol.* **2006**, *1*, 103−111.
(26) Bush, A. I.; Tanzi, R. E. *Neurotherapeutics* **2008**, *5*, 421−432.
(27) Kozlowski, H.; Luczkowski, M.; Remelli, M.; Valensin, D. *Coord. Chem. Rev.* **2012**, *256*, 2129−2141.
(28) Grasso, G.; Giuffrida, M. L.; Rizzarelli, E. *Metallomics* **2012**, *4*, 937−949.
(29) Grasso, G.; Salomone, F.; Tundo, G. R.; Pappalardo, G.; Ciaccio, C.; Spoto, G.; Pietropaolo, A.; Coletta, M.; Rizzarelli, E. *J. Inorg. Biochem.* **2012**, *117*, 351−358.
(30) Grasso, G.; Pietropaolo, A.; Spoto, G.; Pappalardo, G.; Tundo, G. R.; Ciaccio, C.; Coletta, M.; Rizzarelli, E. *Chem.—Eur. J.* **2011**, *17*, 2752−2762.
(31) Marx, G.; Gilon, C. *ACS Chem. Neurosci.* **2012**, *3*, 633−642.
(32) Berg, J. M.; Shi, Y. *Science* **1996**, *271*, 1081−1085.
(33) Takeda, A. *Brain Res. Brain Res. Rev.* **2000**, *34*, 137−148.
(34) Frederickson, C. J.; Koh, J. Y.; Bush, A. I. *Nat. Rev. Neurosci.* **2005**, *6*, 449−462.
(35) Qian, J.; Noebels, J. L. *J. Physiol.* **2005**, *566*, 747−758.
(36) Takeda, A.; Fuke, S.; Ando, M.; Oku, N. *Neuroscience* **2009**, *158*, 585−591.
(37) Sindreu, C.; Storm, D. R. *Front. Behav. Neurosci.* **2011**, *5*, 68.
(38) Bhatnagar, S.; Taneja, S. *Br. J. Nutr.* **2001**, *85* (Suppl2), S139−S145.
(39) Yang, Y.; Jing, X.-P.; Zhang, S.-P.; Gu, R.-X.; Tang, F.-X.; Wang, X.-L.; Xiong, Y.; Qiu, M.; Sun, X.-Y.; Ke, D.; Wang, J.-Z.; Liu, R. *Plose One 8* **2013**, e55384.
(40) Sindreu, C.; Palmiter, R. D.; Storm, D. R. *Proc. Natl. Acad. Sci. U.S.A.* **2011**, *108*, 3366−3370.
(41) Leung, K. W.; Liu, M.; Xu, X.; Seiler, M. J.; Barnstable, C. J.; Tombran-Tink, J. *Invest. Ophthalmol. Vis. Sci.* **2008**, *29*, 1221−1231.
(42) Sowa-Kucma, M.; Legutko, B.; Szewczyk, B.; Novak, K.; Znojek, P.; Poleszak, E.; Papp, M.; Pilc, A.; Novak, G. *J. Neural. Transm.* **2008**, *115*, 1621−1628.
(43) Corona, C.; Masciopinto, F.; Silvestri, E.; Viscovo, A. D.; Lattanzio, R.; Sorda, R. L.; Ciavarelli, D.; Goglia, F.; Piantelli, M.; Canzoniero, L. M.; Sensi, S. L. *Cell Death Dis.* **2010**, *1*, e91.
(44) Hwang, J. J.; Park, M. H.; Choi, S. Y.; Koh, J. Y. *J. Biol. Chem.* **2005**, *280*, 11995−12001.
(45) Hwang, I. Y.; Sun, E. S.; An, J. H.; Im, H.; Lee, S. H.; Lee, J. Y.; Han, P. L.; Koh, J. Y.; Kim, Y. H. *J. Neurochem.* **2011**, *118*, 855−863.
(46) Travaglia, A.; Pietropaolo, A.; La Mendola, D.; Nicoletti, V. G.; Rizzarelli, E. *J. Inorg. Biochem.* **2012**, *111*, 130−137.
(47) Ross, G. M.; Shamovsky, I. L.; Lawrance, G.; Solc, M.; Dostaler, S. M.; Jimmo, S. L.; Weaver, D. F.; Riopelle, R. J. *Nat. Med.* **1997**, *3*, 872−878.
(48) Wang, W.; Post, J. I.; Dow, K. E.; Shin, S. H.; Riopelle, R. J.; Ross, G. M. *Neurosci. Lett.* **1999**, *259*, 115−118.
(49) Maitra, R.; Shamovsky, I. L.; Wang, W.; Solc, M.; Lawrance, G.; Dostaler, S. M.; Ross, G. M.; Riopelle, R. J. *Neurotox. Res.* **2000**, *2*, 321−341.
(50) Shamovsky, I. L.; Ross, G. M.; Riopelle, R. J.; Weaver, D. F. *J. Am. Chem. Soc.* **1999**, *121*, 9797−9806.
(51) Travaglia, A.; Arena, G.; Fattorusso, R.; Isernia, C.; La Mendola, D.; Malgieri, G.; Nicoletti, V. G.; Rizzarelli, E. *Chem.—Eur. J.* **2011**, *17*, 3726−3738.
(52) Travaglia, A.; La Mendola, D.; Magrì, A.; Nicoletti, V. G.; Pietropaolo, A.; Rizzarelli, E. *Chem.—Eur. J.* **2012**, *18*, 15618−15631.
(53) Stanzione, F.; Esposito, L.; Paladino, A.; Pedone, C.; Morelli, G.; Vitagliano, L. *Biophys. J.* **2010**, *99*, 2273−2278.
(54) Colangelo, A. M.; Bianco, M. R.; Vitagliano, L.; Cavaliere, C.; Cirillo, G.; De Gioia, L.; Diana, D.; Colombo, D.; Redaelli, C.; Zaccaro, L.; Morelli, G.; Papa, M.; Sarmientos, P.; Alberghina, L.; Martegani, E. *J. Neurosci.* **2008**, *28*, 2698−2709.
(55) Travaglia, A.; Satriano, C.; Giuffrida, M. L.; La Mendola, D.; Rampazzo, E.; Prodi, L.; Rizzarelli, E. *Soft Matter* **2013**, *9*, 4648−4654.
(56) La Mendola, D.; Magrì, A.; Campagna, T.; Campitiello, M. A.; Raiola, L.; Isernia, C.; Hansson, Ö.; Bonomo, R. P.; Rizzarelli, E. *Chem.—Eur. J.* **2010**, *16*, 6212−6223.
(57) Cavanagh, J.; Fairbrother, W.; Palmer, A. G., III; Skelton, N. J. *Protein NMR Spectroscopy: Principles and Practice*; Academic Press: San Diego, CA, 1996.
(58) Hwang, T. L.; Shaka, A. J. *J. Magn. Reson. A* **1995**, *112*, 275−279.
(59) Bartels, C.; Xia, T.; Billeter, M.; Guntert, P.; Wüthrich, K. *J. Biomol. NMR* **1995**, *6*, 1−10.
(60) Stejskal, E. O.; Tanner, J. E. *J. Chem. Phys.* **1965**, *42*, 288−292.
(61) La Mendola, D.; Magrì, A.; Hansson, Ö.; Bonomo, R. P.; Rizzarelli, E. J. *Inorg. Biochem.* **2009**, *103*, 758−765.
(62) Gans, P.; Sabatini, A.; Vacca, A. *Talanta* **1996**, *43*, 1739−1753.
(63) Alderighi, L.; Gans, P.; Ienco, A.; Peters, D.; Sabatini, A.; Vacca, A. *Coord. Chem. Rev.* **1999**, *184*, 311−318.
(64) Frisch, M. J. et al. *Gaussian 03*; Gaussian, Inc.: Wallingford, CT, 2004.
(65) Becke, A. D. *J. Chem. Phys.* **1993**, *98*, 5648−5652.
(66) Becke, A. D. *J. Chem. Phys.* **1993**, *98*, 1372−1376.
(67) Becke, A. D. *Phys. Rev. A* **1988**, *38*, 3098−3100.
(68) Lee, C.; Yang, W.; Parr, R. G. *Phys. Rev. B* **1988**, *37*, 785−789.
(69) Schäfer, A.; Huber, C.; Ahlrichs, R. *Chem. Phys.* **1994**, *100*, 5829−5835.
(70) Wüthrich, K. *NMR of Proteins and Nucleic Acids*; Wiley: New York, 1986.

(71) Joszai, V.; Nagy, Z.; Osz, K.; Sanna, D.; Di Natale, G.; La Mendola, D.; Pappalardo, G.; Rizzarelli, E.; Sovago, I. *J. Inorg. Biochem.* **2006**, *100*, 1399−1409.
(72) Altun, Y.; Köseoglu, F. *J. Solution Chem.* **2005**, *34*, 213−231.
(73) Myari, A.; Malandrinos, G.; Plakatouras, J.; Hadjiliadis, N.; Sovago, I. *Bioinorg. Chem. Appl.* **2003**, *1*, 99−112.
(74) Kallay, C.; Osz, K.; David, A.; Valastyan, Z.; Malandrinos, G.; Hadjiliadis, N.; Sovago, I. *Dalton Trans.* **2007**, 4040−4047.
(75) Kozlowski, H.; Bal, W.; Dyba, M.; Kowalik-Jankowska, T. *Coord. Chem. Rev.* **1999**, *184*, 319−346.
(76) Torok, I.; Gadja, T.; Gyurcsik, B.; Toth, G. K.; Peter, A. *J. Chem. Soc., Dalton Trans.* **1998**, 1205−1212.
(77) Myari, A.; Malandrinos, G.; Deligiannakis, Y.; Plakatouras, J. C.; Hadjiliadis, N.; Nagy, Z.; Sovago, I. *J. Inorg. Biochem.* **2001**, *85*, 253−261.
(78) Arena, G.; Fattorusso, R.; Grasso, G.; Grasso, G. I.; Isernia, C.; Malgieri, G.; Milardi, D.; Rizzarelli, E. *Chem.—Eur. J.* **2011**, *17*, 11596−11603.
(79) Corniola, R. S.; Tassabehji, N. M.; Hare, J.; Sharma, G.; Levenson, C. W. *Brain Res.* **2008**, *1237*, 52−61.
(80) Alam, S.; Kelleher, S. L. *Nutrients* **2012**, *4*, 875−903.
(81) Adamo, A. M.; Zago, M. P.; Mackenzie, G. G.; Aimo, L.; Keen, C. L.; Keenan, A.; Oteiza, P. I. *Neurotox. Res.* **2010**, *17*, 1−14.
(82) Mineo, P.; Vitalini, D.; La Mendola, D.; Rizzarelli, E.; Scamporrino, E.; Vecchio, G. *J. Inorg. Biochem.* **2004**, *98*, 254−265.